

Tina Memo No. 2005-007
Work submitted to IPMI 2005
Published at MICCAI 2005

Robust Tissue Boundary Detection for Cerebral Cortical Thickness Estimation

M.L.J. Scott and Dr. N.A. Thacker

Last updated
23 / 02 / 2005



Imaging Science and Biomedical Engineering Division,
Medical School, University of Manchester,
Stopford Building, Oxford Road,
Manchester, M13 9PT.

Abstract

This paper presents an algorithm for determining regional cerebral grey matter cortical thickness from magnetic resonance scans. In particular, the modification of a gradient-based edge detector into an iso-grey-level boundary detector to reliably determine the low-contrast grey-white matter interface is described and discussed. The reproducibility of the algorithm over 31 gyral regions is assessed using repeat scans of four subjects, and a technique for correcting the misplacement of the grey-white matter boundary is shown to significantly reduce the systematic error on the reproducibility.

1 Introduction

The determination of human cerebral cortical grey matter thickness has enormous potential use in the assessment of both pathology and the processes of normal brain maturation and ageing. Grey matter (GM) volume loss is seen throughout adulthood to old age [1] and cortical thinning has been shown to occur at a greater rate in males than in females [2]. Loss of GM volume, and increased cortical thinning relative to control subjects has been implicated in various degenerative and developmental diseases, such as Alzheimer's disease [3], Huntington's Chorea [4], Multiple Sclerosis [5] and Schizophrenia [6], whereas focal increases in GM have been observed in the elderly depressed [7]. The characterisation of cortical thickness patterns in terms of normal ageing, disease, disease severity and disease progression should provide a valuable resource for the assessment of rate and severity of pathological processes.

The highly convoluted folding of the cortex provides two specific challenges to the estimation of thickness. The first is the problem of how to measure a thickness of a curved structure, the second is the determination of the boundaries of the GM ribbon, particularly when the opposing banks of two gyri are sufficiently close that there is no cerebro-spinal fluid (CSF) between them, or when two sulci have no intervening white matter (WM). These problems are often obviated by using a surrogate measure of thickness, such as probabilities of tissue occurrence [8] or measures of GM density (eg, [1]) typical of Voxel Based Morphology (VBM) methods [9]. The main difficulties with these techniques have been well discussed in the literature [10] [11]. Aside from the statistical difficulties associated with forming valid conclusions when using VBM-style methods, the variation in topological structure confounds the interpretation of the most significant volumetric changes.

Assuming for the moment that the GM/WM and GM/CSF boundaries have been accurately segmented in 3D, there are various measures of distance between the two surfaces that might be employed. First, if an active shape model algorithm using correspondences (eg. [12]) has been used to create the surfaces, the distance between the corresponding points on the two surfaces can be used. However, anatomical homology within a group of subjects will not be precise. Secondly, the minimum distance between a given point on one surface and the closest point on the opposing surface can be used. Thirdly, the distance along the surface normal from a point on the first surface to the second surface can be used. Of these two latter methods, the surface normal is the least biased, whereas the minimum distance will always produce a shorter average cortical thickness than the surface normal method [12]. However, with both of the second and third methods, the answer obtained is not directly equivalent as the line paths selected do not coincide.

Another problem with using start points and lines from one surface to the other is that of the degree of curvature of the GM and spacing of the start points. When traversing the GM starting at the GM/WM boundary using equally spaced points along the boundary as the starting points and assuming that surface normals are used, then the curved sulcal fundi will always be oversampled, and the gyral crowns undersampled relative to a flat section of cortex, which will bias a mean result if there are any gyral/sulcal differences in thickness. Indeed, a decrease in cortical thickness is seen with sulcal depth by both Fischl & Sereno (2000) [13] and Jones et al. (2000) [14]. The effect of the bias would be less severe if the median was taken rather than the mean, providing that it was taken over a sufficiently small cortical region.

One very elegant solution to these problems is to use Laplace's equation, as detailed in [14], to calculate diffeomorphic field lines through the cortex. The thickness of the cortex at any given point now becomes the sum of the lengths of the surface normals at each field line, where the start point at each field line is the end point of the surface normal from the previous field line. This ensures that every point has a unique and reversible point on the opposing surface. The assumed model also has some analogy with reality [15], where the cortical mantle is divided into 6 laminar layers. However, the approach has the disadvantage that complete detection of the opposing boundaries is required, which can be a real problem in relatively low resolution data (such as is obtained using magnetic resonance imaging (MRI) with partial volume effects).

The second problem to be addressed is that of determining the GM cortical ribbon boundaries with the underlying WM and enveloping CSF. Segmentation of the tissues requires knowledge of the expected grey-level intensity values

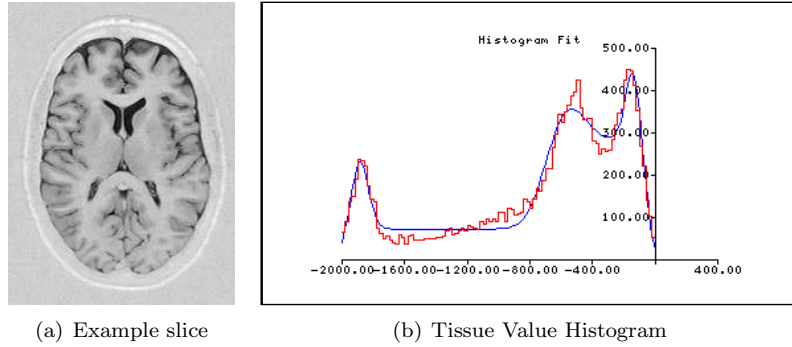


Figure 1: Example axial inversion-recovery image and corresponding grey-level intensity histogram showing, from left to right, peaks for the CSF, GM and WM.

for these tissues. The work presented in this paper makes use of MRI to obtain the anatomical images from which cortical thickness is determined, therefore it is expedient to mention MR-related issues with the mean tissue value estimation and segmentation:

1. The contrast between the tissues needs to be sufficient in order to define a boundary. Normal ageing and disease processes that result in demyelination of the axons of the WM neurones will make the WM appear more like the non-myelinated GM, making accurate boundary detection less feasible;
2. The segmentation used must be able to detect partial voluming of tissues and appropriate boundaries should be located under such circumstances;
3. Through-plane magnetic field inhomogeneities may result in the tissues having different mean values in each imaged slice. Typically it is assumed that the values of the pure tissues are in a set ratio, and that the brain voxel value distribution can be normalised to a given value for one tissue type (eg, of GM [14], or WM [16]).

The simplest model for boundary determination between two tissues (WM/ GM or GM/CSF) is based upon the assumption of a linear image formation process, such that the boundary occurs at the position where the image grey-level intensity is half-way between the two pure tissue values. As can be seen from fig. 1(b) the separation between the mean tissue values for CSF and GM is large (≈ 1300 grey-levels), whereas the separation between GM and WM is much smaller at ≈ 400 grey levels. Therefore, the contrast at the GM/CSF boundary is large and it might be possible to use an edge detector to determine this boundary. However, the contrast at the GM/WM boundary is comparable to the noise in the image, so an edge detector could not be used reliably here. As part of the description for an original cortical thickness estimation algorithm, this paper describes a modification to the Canny edge detector [17] for the determination of the GM/WM boundary. The technique allows an assessment of the accuracy of the boundary positioning, and hence a post-processing correction mechanism for the regional thickness estimates. A reproducibility study is presented, showing that the boundary correction can indeed be used to reduce the systematic error on the cortical thickness measurements.

2 Materials and Methods

2.1 Approach taken to determine cortical thickness

The approach taken here to determine estimates of regional cortical thickness is more straightforward than the elaborate methods typically employed to produce surface rendered/expanded cortical thickness representations [16]. However, the method used results in excellent statistical error and gives physiologically plausible results.

The analysis of the data can be divided into two stages, the pre-processing to convert the original volume of data into the required form and the actual cortical thickness estimation. Initially, the average and standard deviation of the grey-level values of the pure tissues (in this case only GM, WM and CSF are considered) in the image volume are determined for use in future processing steps. grey-level intensity values from a region in the frontal lobe, which is representative of the pure tissue values, are histogrammed (as shown in fig. 1(b)) and a Bayesian mixture model [18], containing terms for both pure tissues and partial volumes, is fitted to the histogram using simplex to obtain the means and standard deviations. The region used encompasses several slices, such that

through-plane inhomogeneities that are present are averaged to some degree. Next, in order to obtain a finer through-plane resolution, the data is up-interpolated in the z-direction [19]. This step is performed explicitly in order to preserve the tissue boundaries in the resultant images, which is done by using a partial volume scheme to provide a constraint on the potential boundaries separating the two tissues that could pass through a partial volume voxel. Boundary orientation can be determined using spatial differentiation of the grey-levels. The volume of data is then registered to a common stereotaxic space (the Talairach atlas [20]) using a linear affine transform. The atlas defines the 31 cortical regions (see table 2 for region names) used later in producing regional histograms of the cortical thickness. The last pre-processing stage is the segmentation of the GM, again using the mean and standard deviation of the pure tissue values. The segmented GM (in the form of the most likely volume estimate for GM in each voxel given the data, based on the defined probability density functions of the image intensity distribution) is used in the cortical thickness estimation.

The cortical thickness estimation itself proceeds by using a modified edge detection process (see below) to determine the GM/WM boundary. The surface normal to the boundary in 3D at each voxel on the boundary is determined, using a 3D Gaussian smoothed data set in order to reduce the effects of noise in the data, and a search is performed over 20mm in this direction on the segmented GM map until an edge (of some description) is found. The type of edge (a CSF edge or WM edge if there is no CSF between opposing banks of a sulcus) is determined using the up-interpolated grey-level data, and the cortical thickness is inserted into the appropriate regional histogram according to the registration into stereotaxic space determined earlier. The median of each regional histogram is calculated in order to give a robust estimation of the average cortical thickness for each region.

2.2 Modification to the Canny edge detector

The approach to thickness measurement presented here is inherently feature based and the GM/WM boundary is of particular importance. Feature detectors generally combine an enhancement stage with a threshold. Statistically, this can be interpreted as performing a hypothesis test, and this leads to the standard problems associated with such tests. Typically, a feature may be present but not detected. Conventional edge detectors are particularly poor at identifying edge boundaries where the boundary contrast approaches the noise level, such as found at the GM/WM boundary. However, medical images have one feature which can be exploited in that the boundary is expected to have one consistent grey-level value. Defining the boundary at the average of the two pure tissue (50% transition) values, it is possible to produce a simple ‘z-score’ measure of each voxel’s grey-level being consistent with this midpoint value. This can be used as the basis for the enhancement process rather than a conventional (summed squares) gradient based measure. Subsequent stages of the detection process can be applied as before. Our implementation is based upon a simplified version of the Canny edge detector. This new iso-contour Canny (or Iso-Canny) algorithm has the advantage that although noise processes may move the position of the detected boundary, these processes cannot prevent detection of a transition. A surrogate of the probability of a grey-level being consistent with the expected boundary value is modelled as a Gaussian with a standard deviation of 10 times that of the noise in the input image. This is monotonically related to a true hypothesis probability, but has better numerical properties for subsequent processing and sub-voxel peak location.

The later stages of the standard Canny edge detector perform non-maximal suppression and hysteresis thresholding which results in well localised connected edge strings which persist into low edge strength regions. Edge locations are computed within each slice of the data to sub-pixel accuracy from quadratic fits to the peak in the edge strength map. This is necessary in order to attempt to measure cortical thickness changes of the order of a fraction of a millimetre. Typical performance of these techniques results in approximately 0.1 mm reproducibility.

The Iso-Canny routine is applied sequentially in 2D to each up-interpolated slice of the image volume. It could be argued that the boundary should be found within the 3D volume rather than the 2D slice, but in using a 2D method the same boundary is found but merely sampled at the centre of the voxel in the z-direction. Spurious edges detected between the CSF and background are removed by automated masking.

This whole process is particularly reliant on the assumption that one accurately determined boundary value is applicable in all parts of the image volume. The following section describes the implementation of a quality control process which histograms the average grey-level found on either side of the boundary. Shifts in this histogram between regions or datasets can be used to assess systematic errors in the analysis, or failure of the calibration process.

2.3 Post-processing to determine “correct” boundary position

The largest source of systematic error in the thickness estimation is expected to be associated with the determination of the GM/WM boundary location. Here small changes in estimated mean tissue values will have the largest

potential effect on the partial volume interpretation (by at least a factor of 4). This will produce systematic errors on the cortical thickness in all regions when an incorrect grey-level value for the midpoint of the grey and white matter is used. Presented here is a technique for monitoring this effect and for correcting for it *post hoc* if required.

In order to calibrate such a correction for a given subject and using in each case the same set of grey-level and probability images, the effect on the median thickness in each region by perturbing the GM/WM grey-level midpoint by -80 to +80 (in increments of 20 grey-levels) was investigated. The regression coefficients of median thickness against grey-level perturbation are presented in table 2.

The GM/WM boundary should be a step edge, the width of which should not extend over many pixels. Therefore if the image volume is traversed from the edge position (using what is believed to be the correct GM/WM midpoint) along the previously determined orientation, in both the positive and negative direction by 2mm, one would expect to be within pure tissue (grey and white depending upon the direction). Assuming that the image gradient is the same either side of the edge boundary, it is expected that the value at the edge (ie. at the central position) will be half way between the values 2mm away either side, using linear interpolation. The difference between the two values is therefore the offset by which the edge has been incorrectly placed, as illustrated in fig. 2.

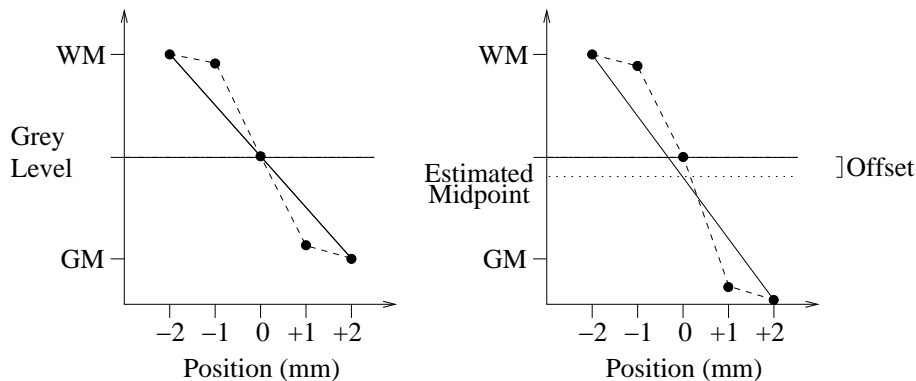


Figure 2: Diagram illustrating the midpoint offset calculation. The plots show position on the x-axis and grey-level on the y-axis. Marked are the pure tissue grey-level values for GM and WM and the midpoint between them is shown by the dash-dot line. The central position is at the midpoint (edge) and the two positions on each side are in GM and WM. The left-hand plot shows the ideal case, where the linear interpolation (solid line) between the grey-level values of the positions 2mm either side corresponds to the midpoint value. The right-hand plot shows an example of the case where the value of the position in the GM is less than the pure tissue value, so that the interpolated grey-level value at the central position is less than the midpoint (edge) value.

In order to obtain a value for each region, the average grey-level at each tissue boundary location in the region is entered into a histogram. The peak of the histogram is taken as the offset estimate. This grey-level offset corresponds to an equivalent median thickness error, which can be calculated using the appropriate regression coefficients (given in table 2) as determined earlier.

3 Subjects and Scan Parameters

4 normal volunteers (all male, ages: 34, 40, 40, 46) all underwent MR scans on two occasions within 7-21 days apart. All scans were performed in the morning, at approximately the same time of day for each subject. All subjects gave informed consent and the study was approved by the Central Manchester Local Research Ethics Committee. All scans were performed using a 1.5 Tesla whole-body scanner (Philips ACS PT 6000 NT, Philips Medical Systems, Best, The Netherlands) with a quadrature birdcage headcoil. An axial anatomical inversion recovery sequence was acquired (TI/TR/TE=300/6850/18ms, 90° flip angle, echo train length=9, matrix size=256², in-plane resolution=0.898²mm, slice thickness=3.0mm, 51 slices taken covering the whole of the brain).

These images were used to determine GM thickness in 31 cortical regions, as described above. Reproducibility of the technique was assessed by comparison of the regional median thicknesses of the two acquisitions from each subject. The subject with the worst reproducibility underwent the correction for the misplacement of the Iso-Canny boundary, and the reproducibility of the modified results was assessed.

4 Results

4.1 Reproducibility results

Figure 3 shows a scatterplot of the reproducibility results. The 31 regional cortical thickness estimates from the 2nd scan are plotted against those of the first, for all four subjects. Table 1 gives the corresponding regression coefficients, and the standard error on their measurement for the 4 subjects. Subjects 2, 3 and 4 have slopes which lie within 5% of the expected value of 1, whereas subject 1 shows a 16% error. The systematic error on the thickness measurements for this group is calculated as the RMS of the differences between the line of equality and the coefficients, scaled by $\sqrt{2}$ to account for the fact two measurements have been taken, and amounts to 6.2% on the measurement in any given individual. The main cause of this bias is in the determination of the Bayesian prior terms, the means and the standard deviations of the CSF, GM and WM peaks.

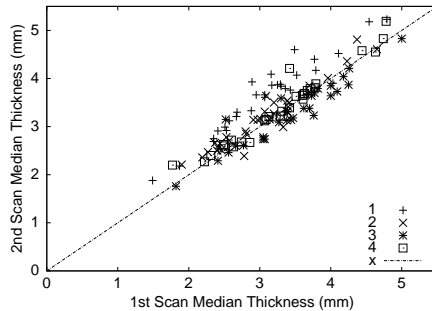


Figure 3: Scatterplot of 2nd vs 1st scan cortical thickness measurements for 31 regions in each of 4 subjects. The line of equality is also shown.

Table 1: Table of fitted slopes and standard error on the fit for each subject for the data in fig. 3. Note that all regressions are constrained to pass through the origin.

Subject	Slope	Std.Err
1	1.16	0.0148
2	1.04	0.0111
3	0.95	0.0098
4	1.03	0.0088

The standard error of the data about the regression is indicative of the statistical error due to sampling of the thickness distribution on any given region of the data, which can be calculated as the product of the standard error and the \sqrt{N} where N is the number of regions (31). This amounts to no more than 0.06mm.

4.2 Iso-Canny correction results

Table 2 gives, for the two scans of subject 1, the regression coefficients of the slopes of median thickness against the extent of GM/WM midpoint perturbation, as well as the estimated offset values by which the boundary was misplaced. In the majority of regions, the slopes are near perfect negative linear correlations of thickness with midpoint perturbation. The few regions where this is not the case are physically small and have large statistical error. The offset results demonstrate a negative bias (roughly ranging between 0 and -100) which is also seen in a larger cohort (results not shown). This is consistent with the GM grey-levels being lower than expected. The thickness estimation technique assumes that the average of two pure tissue values can be taken as the value at the boundary between these tissues. However, due to the slice thickness of this data, it is likely that there are substantial partial volume effects. GM/CSF partial volumes will result in a more pronounced effect than GM/WM partial volumes, which could explain the peak shift seen in the data. If this is the case, the boundary correction may still be used for correcting the systematic error, even though the peak is no longer expected to be at the same grey-level as the assumed tissue boundary.

Table 2: Table of the Talairach regions investigated, values of the slopes of median thickness against Iso-Canny midpoint used and calculated offset values for the two scans of subject 1.

Lobe	Region	Slope ($\times 10^{-3}$) (mm/grey-level)		Offset (grey-levels)	
		Scan 1	Scan 2	Scan 1	Scan 2
Frontal	Rectal Gyrus	-4.08	-1.64	8.00	-126.67
	Orbital Gyrus	-1.23	-1.08	-173.33	127.62
	Precentral Gyrus	-4.64	-8.26	-23.33	-50.13
	Inferior Gyrus	-4.37	-6.47	-16.57	-67.88
	Middle Gyrus	-4.50	-6.62	-30.14	-74.17
	Superior Gyrus	-4.96	-7.23	-32.64	-82.07
	Medial Gyrus	-4.33	-7.46	-21.78	-48.68
Limbic	Posterior Cingulate	-1.30	-5.28	-10.26	-45.81
	Anterior Cingulate	-6.32	-7.03	-7.27	-47.69
	Subcallosal Gyrus	-2.12	2.82	-126.67	-60.44
Occipital	Inferior Gyrus	-2.24	-4.28	-3.64	-46.67
	Lingual Gyrus	-2.03	-5.03	-19.39	-95.24
	Middle Gyrus	-2.48	-5.09	5.22	-45.46
	Superior Gyrus	-2.04	-4.82	-55.24	-156.00
	Cuneus	-2.67	-5.61	-20.98	-58.24
Parietal	Insula	-3.15	-2.53	-34.02	-72.94
	Angular Gyrus	-3.93	-4.89	-51.43	-99.26
	Supramarginal Gyrus	-3.43	-6.10	-22.22	-52.08
	Cingulate Gyrus	-3.93	-5.03	-18.58	-54.81
	Inferior Lobule	-4.03	-5.79	-20.39	-88.79
	Superior Lobule	-4.33	-5.80	-37.58	-70.77
	Paracentral Lobule	-3.73	-7.26	-110.30	-108.57
	Postcentral Gyrus	-3.92	-6.85	-34.67	-60.61
Precuneus	-3.83	-6.48	-34.29	-67.83	
Temporal	Transverse Gyrus	-5.58	-9.83	8.48	-20.00
	Uncus	-2.23	-1.37	-42.67	-70.83
	Fusiform Gyrus	-1.93	-4.18	-21.40	-65.78
	Inferior Gyrus	-3.07	-2.88	-41.90	-95.76
	Parahippocampal Gyrus	-1.91	-4.23	-18.63	-76.92
	Middle Gyrus	-2.66	-5.45	-22.48	-54.57
	Superior Gyrus	-3.22	-4.21	2.37	-42.46

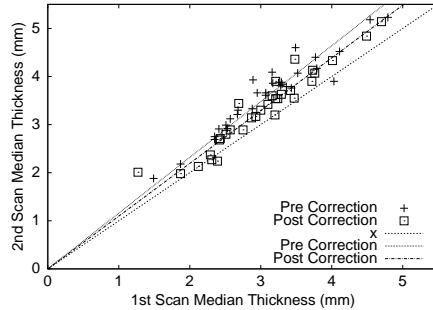


Figure 4: Scatterplot of regional median thickness for the 2nd scan against the 1st scan of subject 1. The scatterplot shows the line of equality, the original reproducibility results from 3 and reproducibility results after applying the Iso-Canny correction to the data.

4.3 Effect of Iso-Canny correction on reproducibility

Figure 4 shows the effect of applying the Iso-Canny offset correction to the regional cortical thickness measurements from both scans of subject 1. Note that the slope of the regression is reduced from 16% greater than unity to 9.7%,

and the standard error on fitting the regression has marginally improved from 0.0148 to 0.0133mm.

5 Discussion

This paper has presented some of the difficulties in reliably determining GM cortical thickness from images obtained using MRI. Descriptions of a cortical thickness algorithm and the required pre-processing stages are given. The method is applied to repeat scans of four young normals, and the reproducibility of the *whole* procedure is assessed. Using these four subjects, it is possible to quantify the systematic error on any region from a given individual at 6.2%. The statistical error on the regional measurements is very much better, at approximately 0.06mm on any given region.

The large systematic error, mainly due to the initial grey-level histogram parameter determination, has implications for the use of this cortical thickness estimation in longitudinal studies. A 6% systematic error would be expected to mask any real changes in cortical thickness over the time scale in which the measurements are likely to be made. However, several steps can be taken in order to achieve greater consistency. Any group wishing to perform such a study would have to ensure an identical scanner set-up, and identical subject physiology. Fixing the Bayesian prior terms and the ratio of grey-level histogram peaks between scans may then help in reducing variability. Note that the natural variation between subjects will be far greater than the effects of the systematic error, such that group-wise comparisons are feasible on tens of subjects. This is a considerable improvement over the use of VBM, which requires hundreds of subjects to produce statistically significant results. However, the ultimate goal of this work is to provide information suitable for decision support in individual subjects. This may yet be achievable with more care over the interpretation of systematic errors and appropriate use of the resulting set of regional thickness measurements.

The main focus of the paper is a description of a GM/WM boundary detector. The advantage of basing this upon a conventional edge detector is that it provides edge locations computed to sub-pixel accuracy, as is necessary when measuring structures as small as the GM ribbon. In addition, well localised connected edge strings persist even in conventional low edge strength regions. The effect of perturbing the GM/WM midpoint value, in order to determine the effect of modifying the position of the GM/WM edge strings on the regional thickness estimation was used to calibrate a regional correction factor. This was used in conjunction with a technique for determining the inaccuracy in the position of the boundary, for the subject with the greatest systematic error, in order to produce a distance by which the regional thickness was in error. The modified regional estimates were then used to assess any change in reproducibility afforded by the boundary correction technique.

The technique improved the systematic error in all 31 regions of subject 1 from 16% to 9%, so the technique appears to be beneficial. However, this error is still greater than that exhibited by the other three subjects, probably for reasons associated with the segmentation. First, if the tissue value estimations led to inaccuracies in the GM/WM boundary, then the GM/CSF boundary found on the segmented GM maps may also have been inaccurate, although as commented in the introduction, misplacement of the GM/CSF boundary by 50 grey-levels or so will have a much smaller effect on the median thickness than misplacing the GM/WM boundary by the same amount.

6 Acknowledgements

This work was supported by a grant from the Wellcome Trust. Thanks to Prof. A. Jackson and Prof. P. Rabbitt for the subject data and Dr. Paul Bromiley for the segmentation code.

References

- [1] Sowell, E.R., Petersen B.S., Thompson P.M. et al: Mapping cortical change across the human life span. *Nature Neuroscience* **6** (2003) 309–315
- [2] Magnotta V.A., Andreasen N.C., Schultz S.K., Harris G. et al: Quantitative in vivo measurement of gyrification in the human brain: changes associated with aging. *Cereb. Cortex* **9** (1999) 151–160
- [3] Double K.L., Halliday G.M., J J Krill J.J., Harasty J.A. et al: Topography of brain atrophy during normal aging and Alzheimer’s disease. *Neurobiol. Aging* **17** (1996) 513–521
- [4] Rosas H.D., Liu A.K., Hersch S., Glessner M., Ferrante R.J. et al: Regional and progressive thinning of the cortical ribbon in Huntington’s disease. *Neurol.* **58** (2002) 695–701

- [5] Sailer M., Fischl B., Salat D., Tempelmann C. et al: Focal thinning of the cerebral cortex in multiple sclerosis. *Brain* **126** (2003) 1734–1744
- [6] Kuperberg G.R., Broome M.R., McGuire P.K., David A.S. et al: Regionally localized thinning of the cerebral cortex in schizophrenia. *Arch. Gen. Psychiatry* **60** (2003) 878–888
- [7] Ballmaier M., Sowell E.R., Thompson P.M., Kumar A. et al: Mapping brain size and cortical grey matter changes in elderly depression. *Biol. Psychiatry* **55** (2004) 382–389
- [8] Miller M.I., Massie A.B., Ratnanather T., Botteron K.N., Csernansky J.G.: Bayesian construction of geometrically based cortical thickness metrics. *NeuroImage* **12** (2000) 676–687
- [9] Good C.D., Johnrude I.S., Ashburner J., Henson R.N.A. et al: A voxel based morphometric study of ageing in 465 normal adult brains. *NeuroImage* **14** (2001) 21–36
- [10] Bookstein F.L.: “Voxel-based morphometry” should not be used with imperfectly registered images. *NeuroImage* **14** (2001) 1454–1462
- [11] Crum W.R., Griffin L.D., Hill D.L.G., Hawkes D.J.: Zen and the art of medical image registration: correspondence, homology and quality. *NeuroImage* **20** (2003) 1425–1437
- [12] MacDonald D., Kabani N., Avis D., Evans A.C.: Automated 3-D extraction of inner and outer surfaces of cerebral cortex from MRI. *NeuroImage* **12** (2000) 340–356
- [13] Fischl B., Dale A.M.: Measuring the thickness of the human cerebral cortex from magnetic resonance images. *Proc. Nat. Acad. Sci. USA* **97** (2000) 11050–11055
- [14] Jones S.E., Buchbinder B.R., Aharon I.: Three-dimensional mapping of cortical thickness using Laplace’s equation. *Hum. Br. Map.* **11** (2000) 12–32
- [15] Annese J., Pitiot A., Dinov I.D., Toga A.W.: A myelo-architectonic method for the structural classification of cortical areas. *NeuroImage* **21** (2004) 15–26
- [16] Dale A.M., Fischl B., Sereno M.I.: Cortical surface-based analysis I: segmentation and surface reconstruction. *NeuroImage* **9** (1999) 174–194
- [17] Canny J.F.: A Computational Approach to Edge Detection. *Patt. Anal. Mach. Intel.* **8** (1986) 679–698
- [18] Pokrić M., Thacker N.A., Scott M.L.J., Jackson A.: Multi-dimensional medical image segmentation with partial voluming. *Proc. MIUA* **5** (2001) 77–81
- [19] McKie S., Thacker N.A.: Step interpolation of MR images with inter-slice gap correction. *Tina Memo* 2003-010 (2003)
- [20] Talairach J., Tournoux P.: Co-planar stereotaxic atlas of the human brain. 3-dimensional proportional system: An approach to cerebral imaging. Thieme medical publishers (1988)